ISSN 2176-5480

22nd International Congress of Mechanical Engineering (COBEM 2013)
November 3-7, 2013, Ribeirão Preto, SP, Brazil

CONTROL OF AN ELECTROMECHANICAL PUNDULUM EMBARKED WITH MAGNETORHEOLOGICAL FLUID

Angelo Marcelo Tusset
UTFPR - Av. Monteiro Lobato, CP: 20 - 84016-210, Ponta Grossa - PR, Brazil
tusset@ utfpr.edu.br

Wagner Barth Lenz
UTFPR - Av. Monteiro Lobato, CP: 20 - 84016-210, Ponta Grossa - PR, Brazil
wagner_barth@hotmail.com

Vinicius Piccirillo
UTFPR - Av. Monteiro Lobato, CP: 20 - 84016-210, Ponta Grossa - PR, Brazil
piccirillo@utfpr.edu.br

Carlos Eduardo Marques
UNESP - Av. Bela Vista, CP: 13506-700, Rio Claro-SP, Brazil
carlos_e_marques@hotmail.com

José Manoel Balthazar
UNESP - Av. Bela Vista, CP: 13506-700, Rio Claro-SP, Brazil
jmbaltha@rc.unesp.br

Abstract. *This paper presents the control strategies of an electromechanical system with an embarked pendulum using a magnetorheological (MR) fluid. We used two different approaches for modeling and control of the electromechanical pendulum and electrical parts of the force of friction in the pendulum with the MR fluid. First, we have formulated the control problem in order to design the friction force of friction in the pendulum controller. Then the values of the control friction force functions were transformed into electrical control signals. The numerical simulations were provided in order to show the effectiveness of this method for the active control of the pendulum oscillation.*

Keywords: *Electromechanical System; Active Control; Magnetorheological Fluid; Nonlinear Model.*

1. INTRODUCTION

The control of the pendulum embedded by using magneto rheological fluid (MR) brakes proposed in this paper follows the principle using two controls, one feedforward control in order to maintain the system in a desired orbit, and feedback control to take system in the desired orbit (Tusset et al, 2013). The feedback control is obtained using Equation state-dependent Riccati (SDRE).

The SDRE control provides computational algorithms simple and highly effective for the control of nonlinear systems (Fenili and Balthazar, 2011).

MR fluids are composed of micron-sized magnetic particles, located inside a liquid carrier, that form chain-like structures when the external magnetic field is applied, resulting in an increase of the apparent viscosity of the fluid (Avraam et al., 2010).

MR brakes create braking torque by changing the viscosity of the MR fluid inside the axis. In the initial state the fluid has a viscosity similar to low viscosity oil. Upon activation with a magnetic flux, it changes to a thick consistency (Senkal and Gurocak, 2010).

A representation of the embarked pendulum model can be seen in Figure 1:

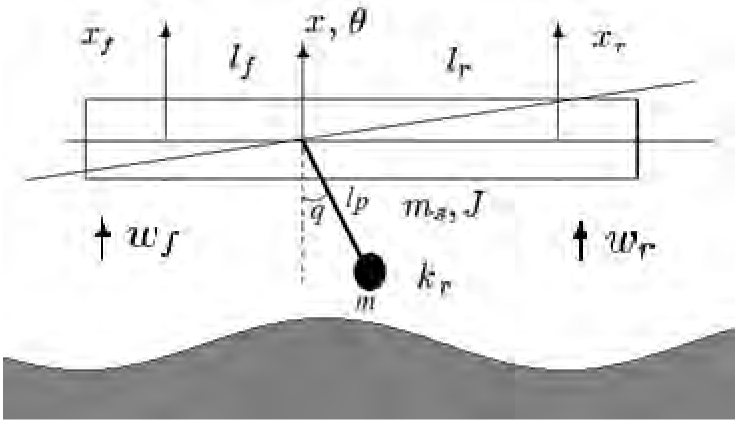

Figure 1. Pendulum embarked model

The model consists of two parts: m_s is the platform mass and m is the pendulum mass, being a system with three degrees of freedom. It is considered that the mass of the platform is a rigid body with pitch and vertical motions. Since x represents the displacement of the center of gravity of the platform, and θ is the pitch angle. The angles of pendulums are represented by q. The back and forth motion represented by x_f and x_r, respectively, are caused by wave motion and can be represented by w_f and w_r, respectively. The environment in which the platform is submerged generates a damping force due to movements of the hull (drift damping hull) and a thrust which can be represented by (F_b) and (F_k), respectively (Faltinsen, 1990).

2. PENDULUM EMBARKED MODEL

The damping forces due to movements of the hull (drift damping hull) may be represented by Eq. (1) and (2):

$$F_{bf} = b_f\left(\dot{x}_f - \dot{w}_f\right) \tag{1}$$

$$F_{br} = b_r\left(\dot{x}_r - \dot{w}_r\right) \tag{2}$$

The thrust forces carried by the hull displacement can be represented by Eq. (3) and (4):

$$F_{ksf} = k_f(x_f - w_f) \tag{3}$$

$$F_{kr} = k_r(x_r - w_r) \tag{4}$$

The vertical force, the force of pitch and force acting on the pendulum can be represented by:

$$\begin{aligned} m_s\ddot{x} &= F_{ms} \\ J\ddot{\theta} &= F_\theta \\ ml_p{}^2\ddot{q} &= F_q \end{aligned} \tag{5}$$

The balance of forces can be written as follows:

$$\begin{aligned} F_{ms} &= -F_{kf} - F_{bf} - F_{kr} - F_{br} \\ F_\theta &= l_f\cos(\theta)(F_{kf} + F_{bf}) - l_r\cos(\theta)(F_{kr} + F_{br}) \\ F_q &= -c\dot{q} - ml_p\ddot{x}\cos q + ml_p\dot{x}\dot{q}\sin q - gml_p\sin q \end{aligned} \tag{6}$$

Substituting Eq. (6) into Eq. (5) yields the system:

ISSN 2176-5480

$$\begin{cases} \ddot{x} = \dfrac{1}{m_s}\left(-F_{kf} - F_{bf} - F_{kr} - F_{br}\right) \\ \ddot{\theta} = \dfrac{1}{J}\left(l_f \cos(\theta)(F_{kf} + F_{bf}) - l_r \cos(\theta)(F_{kr} + F_{br})\right) \\ \ddot{q} = \dfrac{1}{ml_p{}^2}\left(-c\dot{q} - ml_p \ddot{x}\cos q + ml_p \dot{x}\dot{q}\sin q - gml_p \sin q\right) \end{cases} \tag{7}$$

In general, the equations of motion are considered in terms of dimensionless variables, therefore, introducing new variables defined as: $T = \omega_0 t$, $y = \dfrac{x}{x^*}$, $z = \dfrac{\theta}{\theta^*}$ and $v = \dfrac{q}{q^*}$, where: T^*, x^*, θ^* and q^*, are constant, we obtain the system (8) in state space and dimensionless form:

$$\begin{cases} x'_1 = x_2 \\ x'_2 = -\alpha_1 x_{1f} + \alpha_2 w_f - \alpha_3 x_{2f} + \alpha_4 \dot{w}_f - \alpha_5 x_{1r} + \alpha_6 w_r - \alpha_7 x_{2r} + \alpha_8 \dot{w}_r \\ y'_3 = y_4 \\ x'_4 = \cos(x_3)\left(\beta_1 x_{1f} - \beta_2 w_f + \beta_3 x_{2f} - \beta_4 \dot{w}_f - \beta_5 x_{1r} + \beta_6 w_r - \beta_7 x_{2r} + \beta_8 \dot{w}_r\right) \\ x'_5 = x_6 \\ x'_6 = -\delta_1 x_6 - \delta_2 x'_2 \cos x_5 + \delta_3 x_2 x_6 \sin x_5 - \delta_4 \sin x_5 \end{cases} \tag{8}$$

where:

$$\alpha_1 = -\frac{k_f}{\omega_0^2 m_s};\alpha_2 = \frac{k_f}{\omega_0^2 x^* m_s};\alpha_3 = -\frac{b_f}{\omega_0 m_s};\alpha_4 = \frac{b_f}{\omega_0^2 x^* m_s};\alpha_5 = -\frac{k_r}{\omega_0^2 m_s};\alpha_6 = \frac{k_r}{\omega_0^2 x^* m_s};\alpha_7 = -\frac{b_r}{\omega_0 m_s};\alpha_8 = \frac{b_r}{\omega_0^2 x^* m_s}$$

$$\beta_1 = \frac{l_f k_f}{\omega_0^2 J};\beta_2 = -\frac{l_f k_f}{\omega_0^2 \theta^* J};\beta_3 = \frac{l_f b_f}{\omega_0 J};\beta_4 = -\frac{l_f b_f}{\omega_0^2 \theta^* J} b_f;\beta_5 = -\frac{l_r k_r}{\omega_0^2 J};\beta_6 = +\frac{l_r k_r}{\omega_0^2 \theta^* J};\beta_7 = -\frac{l_r b_r}{\omega_0 J};\beta_8 = \frac{l_r b_r}{\omega_0^2 \theta^* J}$$

$$\delta_1 = -\frac{c}{\omega_0 m l_p{}^2};\ \delta_2 = -\frac{x^*}{q^* l_p};\quad \delta_3 = \frac{x^*}{l_p};\quad \delta_4 = -\frac{g}{l_p};\quad x_{1f} = x_1 - w_f - \sigma_1 \sin x_3;\quad x_{1r} = x_1 - w_r + \sigma_2 \sin x_3;$$

$x_{2f} = x_2 - \dot{w}_f - \sigma_1 x_4 \cos x_4$ and $x_{2r} = x_2 - \dot{w}_r + \sigma_2 x_4 \sin x_3$.

2.1 Numerical Simulations

In Figures 2, 3 and 4, we can observe the behavior of the system (8) for the parameters:

$\alpha_1 = 25{,}86207; \alpha_2 = 25{,}86207; \alpha_3 = 0{,}68965; \alpha_4 = 0{,}68965; \alpha_5 = 25{,}86207; \alpha_6 = 25{,}86207, \alpha_7 = 0{,}68965; \alpha_8 = 0{,}68965;$
$\beta_1 = 13{,}63636; \beta_2 = 13{,}63636; \beta_3 = 0{,}36363; \beta_4 = 0{,}36363; \beta_5 = 20{,}45454; \beta_6 = 20{,}45454; \beta_7 = 0{,}54545; \beta_8 = 0{,}54545;$
$\delta_1 = 1; \delta_2 = 1; \delta_3 = 1; \delta_4 = 9.8; \sigma_1 = 1; \sigma_2 = 1.5; w_f = 0.8\sin(3.7699T)$ *and* $w_r = 0.8\sin(3.7699T)$.

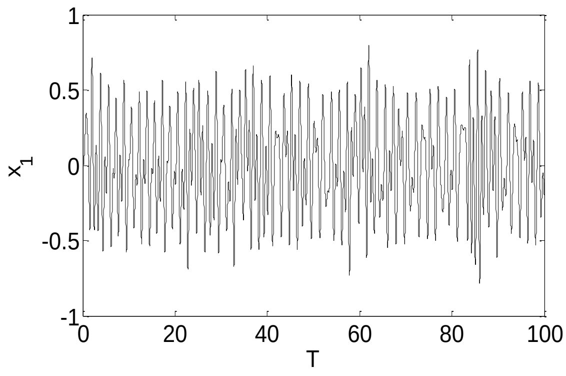

(a)

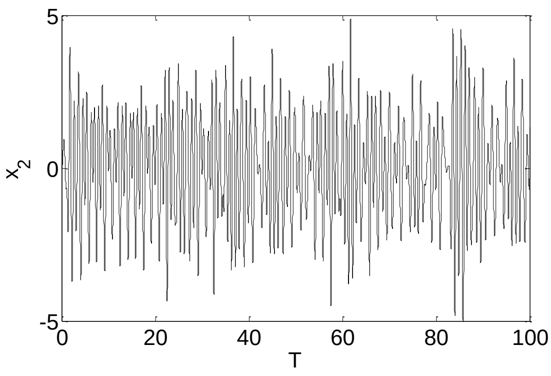

(b)

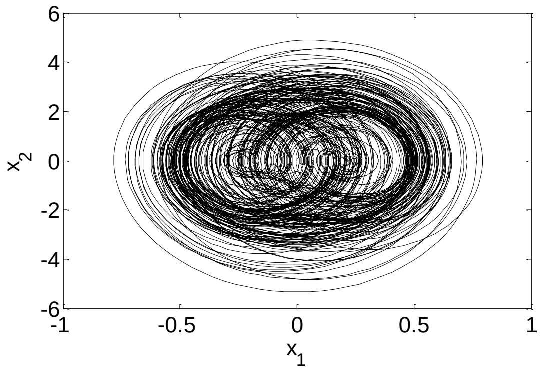

(c)

Figure 2. Vertical movement of the platform: (a) Displacement. (b) Velocity. (c) Phase Diagram

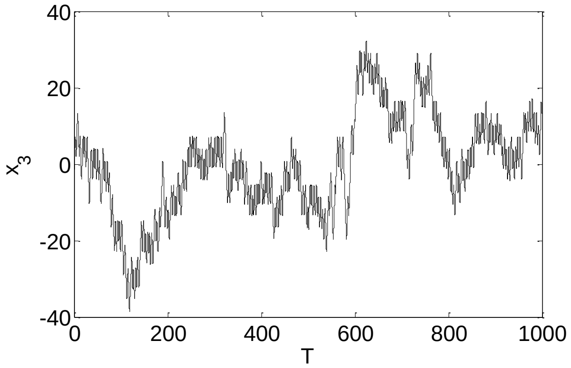

(a)

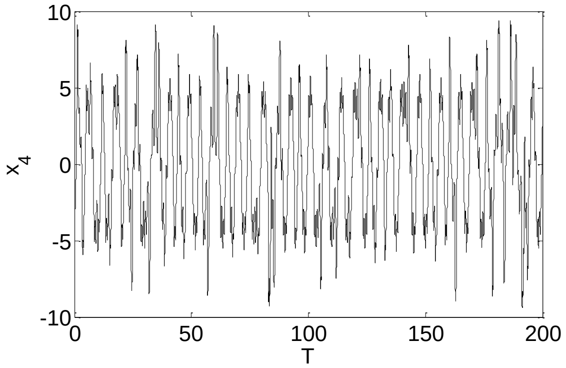

(b)

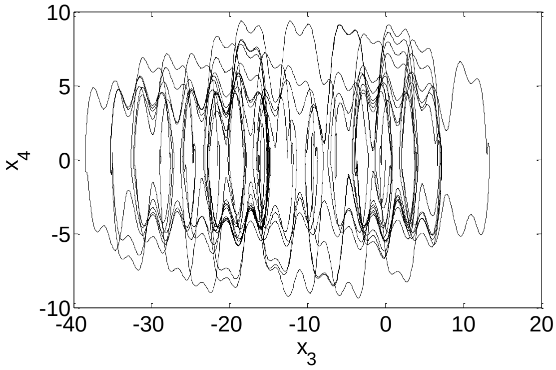

(c)

Figure 3. Pitch movements. (a) Pitch angle. (b) Angular velocity. (c) Phase diagram

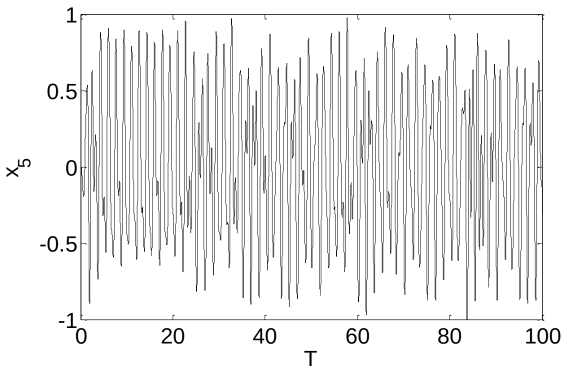

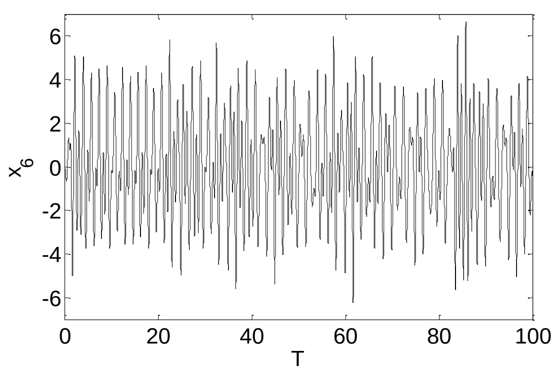

ISSN 2176-5480

(a) (b)

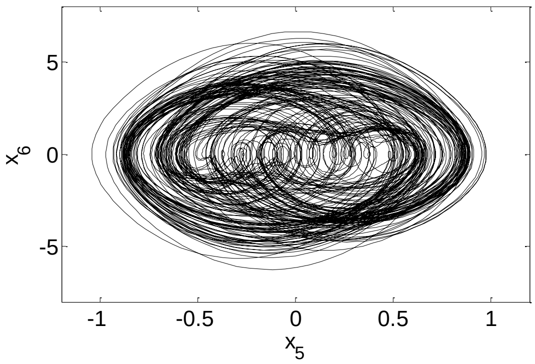

(c)

Figure 4. Movements of the pendulum: (a) Angle of the pendulum (b) Angular velocity. (c) Phase diagram

As can be seen in Figs. 2, 3 and 4 the system exhibits chaotic behavior for these values presented above. In Fig. 5 we can observe the frequency spectrum. Note that, in this case, the behavior of the system is chaotic.

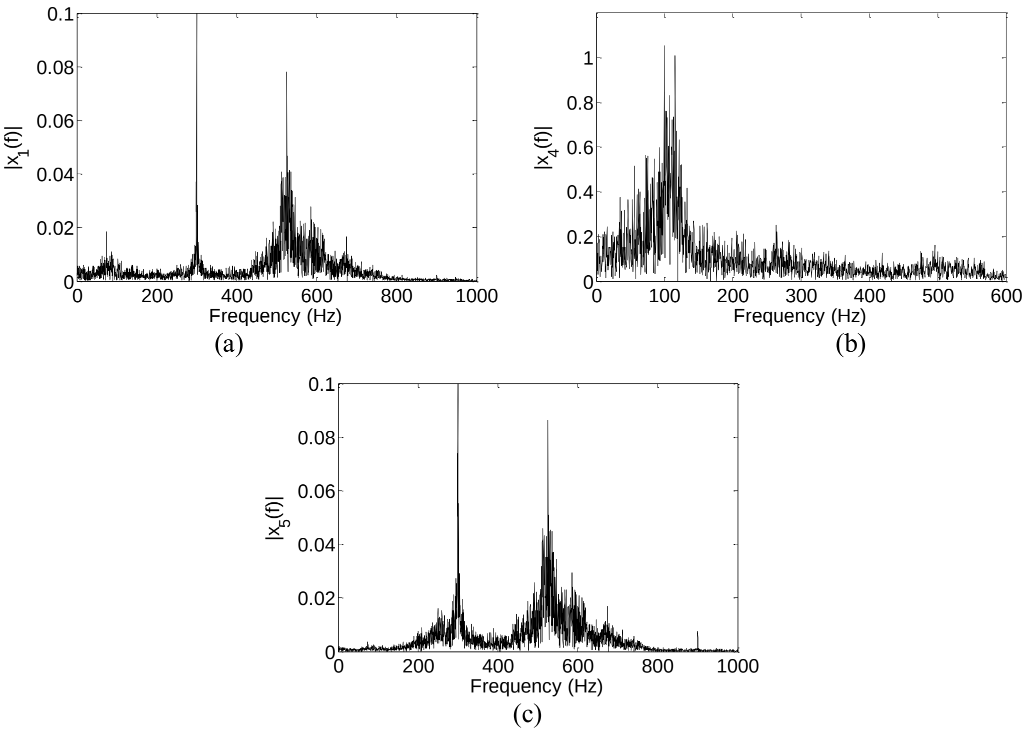

Figure 5. Frequency Spectrum: (a) displacement (x1). (b) Angular pitch velocity. (c) Angle of the pendulum

3. MATHEMATICAL MODEL OF THE TORQUE FOR MR FLUID

MR-brakes have found various applications in many different areas, such as prosthetics, automotive and haptics where the MR-actuator can function as a clutch or brake (Chen and Liao, 2010; Blake and Gurocak 2009; Senkal and Gurocak 2010) .

In Figure 6 we can observe that the torque variation is defined by a positive variation of electric current to MR-brakes.

ISSN 2176-5480

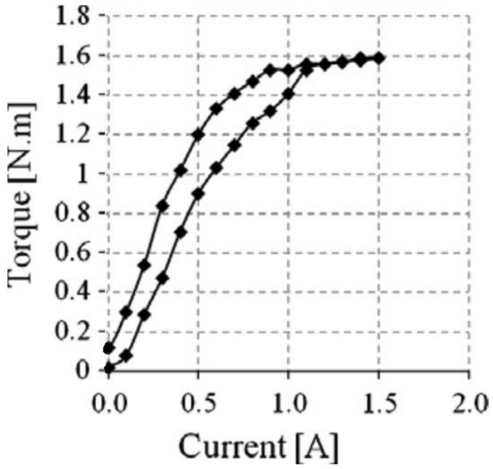

Figure 6. Braking torque versus current (Gonenc and Gurocak, 2012)

For the case of an application as active control is necessary to use the curve energized, because the variations of the power will be used with a frequency, not allowing the de-energizing of the iron used in the brake.

We will consider an approximation, in the form:

$$T(i) = \frac{\gamma_1 e^{\gamma_2 i}}{\gamma_3 e^{\gamma_4 i} + \gamma_5} \tag{9}$$

where: i electric current, e is natural number and $\gamma_1, \gamma_2, \gamma_3, \gamma_4$ and γ_5 are constants, determined by using the least square method (Tusset et al. 2012):

Considering then an approximation function depend on the electric current:

$$T(i) = \frac{0.110759 e^{3.2768 i}}{0.110759 e^{3.2768 i} + 1.6} \tag{10}$$

In Figure 7 one can observe an approach of the Fig. 6 considering the model proposed (10).

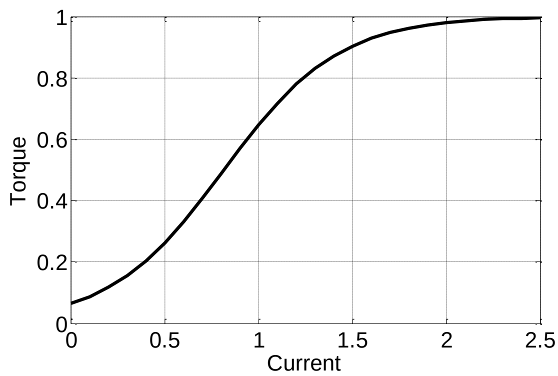

Figure 7. Approach braking torque versus current

4. PROPOST CONTROL FOR PUNDULUM EMBARKED MODEL

Considering the introduction of a controllable Torque (U) in pendulum:

$$\begin{cases} x'_1 = x_2 \\ x'_2 = -\alpha_1 x_{1f} + \alpha_2 w_f - \alpha_3 x_{2f} + \alpha_4 \dot{w}_f - \alpha_5 x_{1r} + \alpha_6 w_r - \alpha_7 x_{2r} + \alpha_8 \dot{w}_r \\ y'_3 = y_4 \\ x'_4 = \cos(x_3)\left(\beta_1 x_{1f} - \beta_2 w_f + \beta_3 x_{2f} - \beta_4 \dot{w}_f - \beta_5 x_{1r} + \beta_6 w_r - \beta_7 x_{2r} + \beta_8 \dot{w}_r\right) \\ x'_5 = x_6 \\ x'_6 = -\delta_1 x_6 - \delta_2 x'_2 \cos x_5 + \delta_3 x_2 x_6 \sin x_5 - \delta_4 \sin x_5 + U \end{cases} \tag{11}$$

where:

$$U = u^* + u \tag{12}$$

The u^* will be the feedforward control and u the feedback control can be determined using SDRE Control (Tusset et al., 2013):

Since the objective of this work is to control x_5 and x_6, in a desired orbit x_5^* and x_6^* the variables x_1, x_2, x_3 and x_4 will be considered only as disturbances of the system.

For the system (11), we have:

$$u^* = \delta_2 x'_2 \cos x_5^* + \delta_4 \sin x_5^* \tag{13}$$

Substituting Eq. (13) in system (8) and considering only the states that wish to control, we have:

$$\begin{cases} x'_5 = x_6 \\ x'_6 = -\delta_1 x_6 + \delta_3 x_2 x_6 \sin x_5 + u \end{cases} \tag{14}$$

Rewriting the system (10) in matrix form: $X = A(x)x + Bu$.

$$\begin{bmatrix} x'_5 \\ x'_6 \end{bmatrix} = \begin{bmatrix} 0 & 1 \\ 0 & -\delta_1 + \delta_3 x_2 \sin x_5 \end{bmatrix} \begin{bmatrix} x_5 \\ x_6 \end{bmatrix} + \begin{bmatrix} 0 \\ 1 \end{bmatrix} u \tag{15}$$

As can be observed in the system (15), the states of the matrix *A(x)* are not controllable and therefore, in order to solve this problem, we consider the introduction of ($x_5 x_6 - x_5 x_6$) in the system (15), resulting in *A(x)* controllable:

$$\begin{bmatrix} x'_5 \\ x'_6 \end{bmatrix} = \begin{bmatrix} 0 & 1 \\ x_6 & -x_5 - \delta_1 + \delta_3 x_2 \sin x_5 \end{bmatrix} \begin{bmatrix} x_5 \\ x_6 \end{bmatrix} + \begin{bmatrix} 0 \\ 1 \end{bmatrix} u \tag{16}$$

The state feedback control law (u) to be considered have the aim to enhance the control performance. In this way, the quadratic cost function for the regulator problem is given by:

$$J = \frac{1}{2} \int_{t_0}^{\infty} \left[x^T Q(x) x + u^T R(x) u \right] dt \tag{17}$$

where $Q(x)$ and $R(x)$ are positive definite matrix.

Assuming full state feedback, the control law is given by:

$$u = -R^{-1}(x) B^T(x) P y \tag{18}$$

where $y = \left[x - x^* \right]$ represents the deviations from the desired trajectory x^*. The State-Dependent-Riccati equation to obtain $P(x)$, is given by:

$$A^T(x)P(x)+P(x)A(x)-P(x)B(x)R^{-1}(x)B^T(x)P(x)+Q(x)=0 \qquad (19)$$

Defining the desired trajectory as the periodic orbit: $x_5^*=0.5\sin(8t)$, and matrices: $Q=\begin{bmatrix}100 & 0\\ 0 & 100\end{bmatrix}$ and $R=[1]$.

In Figure 8 we see the system with the proposed control.

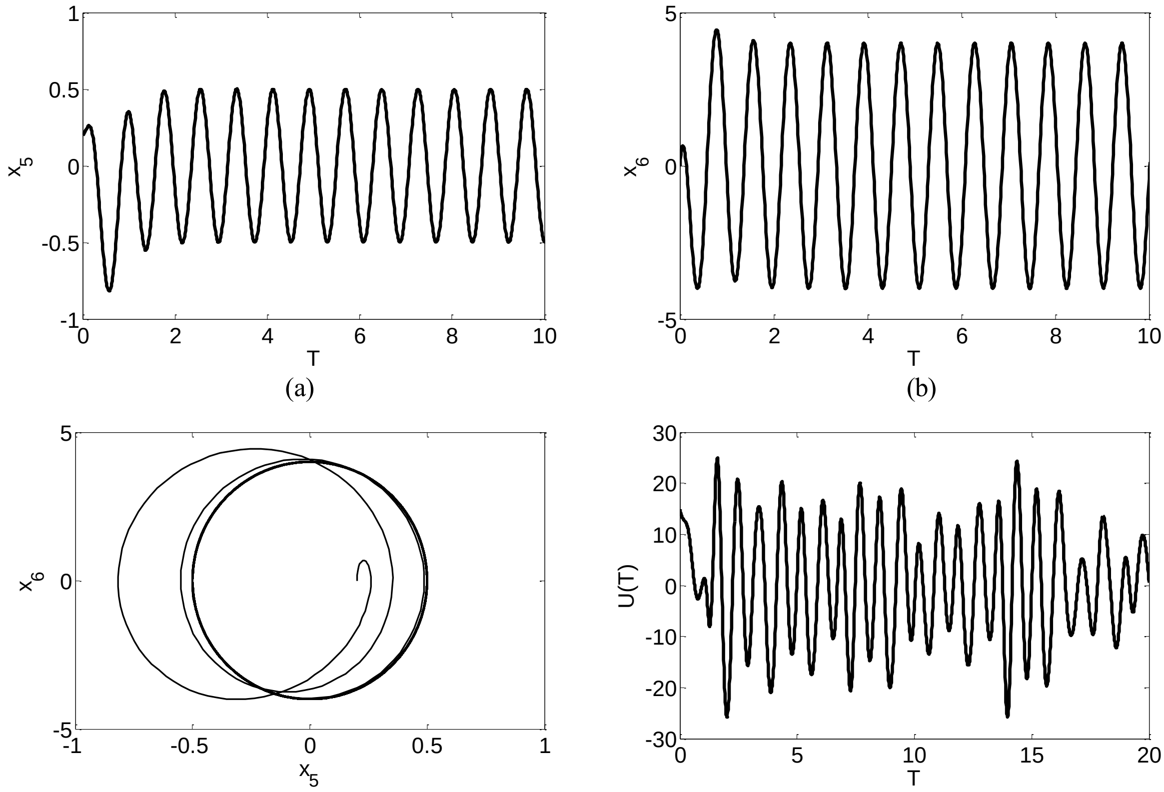

Figure 8. Movements of the pendulum with the proposed control: (a) Angle of the pendulum (b) Angular velocity. (c) Phase diagram. (d) Used torque

As can be seen in Figure 8 the proposed control was effective to control the oscillations of the pendulum (Fig. 8a-c). It can also be seen that to maintain the system in desired orbit the required torque must be variation between positive and negative values. For the case of positive torque should be simply increase the current in the coil until the desired value. On the other hand, in the case of negative torque is necessary to add another clutch assembly is energized 1.5 [A] and reduce torque when needed. Thus when it is desired torque positive energizes a coil of a clutch when torque is needed is negative energizes the coil of the other clutch.

The electrical current to be applied each coil can be determined by solving numerically the following function:

$$C(i)=\frac{0.110759e^{3.2768i}}{0.110759e^{3.2768i}+1.6}-U \qquad (20)$$

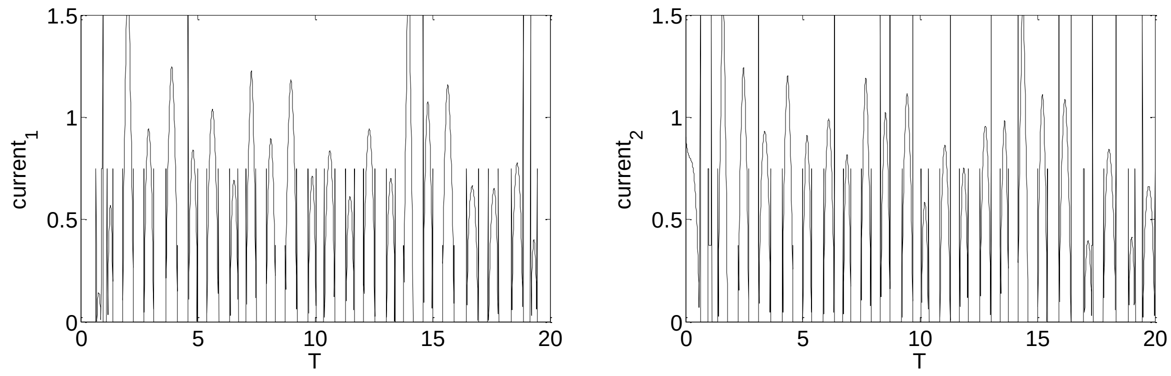

(a) (b)

Figure 9. Current applied: (a) Negative torque. (b) Positive torque

5. CONCLUSIONS

As can be seen in Figures 8 (a), (b) and (c), the chaotic behavior of the pendulum could be steered to a desired periodic orbits ($x_5^* = 0.5\sin(8t)$) with the proposed association of feedforward control (u^*) with feedback (u). Getting the model of the torque-current (20) allowed us to determine the electrical current to be applied to control, as shown in Fig. 9 (a) and (b).

6. REFERENCES

Avraam, M., Horodinca, M., Romanescu, I. and Preumont, A., 2010. “Computer Controlled Rotational MR-brake for Wrist Rehabilitation Device”. *Journal of Intelligent Material Systems and Structures*, Vol. 21, p. 1543-1557.

Faltinsen, O.M., 1990. “Sea Loads on Ships and Offshore Structures”, Cambridge Ocean Technology Series.

Chen, J.Z and Liao, W.H., 2010. “Design, testing and control of a magnetorheological actuator for assistive knee braces”. *Smart Mater Struct*, p. 1-10.

Blake, J. and Gurocak, H., 2009. “*Haptic glove with MR-brakes for virtual reality*”. IEEE/ASME Trans Mechatron, p. 606–615.

Senkal, D. and Gurocak, H. 2010. “Serpentine flux path for high torque MRF brakes in haptics applications”. *Mechatronics*. p. 377–83.

Tusset, A.M., Balthazar, J.M., Felix, J.L.P., 2013. “On elimination of chaotic behavior in a non-ideal portal frame structural system, using both passive and active controls”. Journal of Vibration and Control, Vol. 19, p. 803-813.

Fenili, A. and Balthazar, J.M., 2011. “The rigid-flexible nonlinear robotic manipulator: Modeling and control”. *Communications in Nonlinear Science and Numerical Simulation* Vol. 16, p. 2332–2341.

Tusset, A.M., Balthazar, J.M., Chavarette, F. R. and Felix, J.L.P., 2012. “On energy transfer phenomena, in a nonlinear ideal and nonideal essential vibrating systems, coupled to a (MR) magneto-rheological damper”. *Nonlinear Dynamics*, Vol. 69, p. 1859-1880.

7. RESPONSIBILITY NOTICE

The authors are the only responsible for the printed material included in this paper.